J Mater Sci (2011) 46:6453–6456
DOI 10.1007/s10853-011-5725-z

LETTER

Electrical properties of electrospun carbon nanofibers

Nyle Hedin · Vladimir Sobolev · Lifeng Zhang · Zhengtao Zhu · Hao Fong

Published online: 25 June 2011

Abstract Electrospun carbon nanofibers (ECNs) were prepared through stabilization and carbonization of electrospun polyacrylonitrile nanofibers as the precursor, and their morphological, structural, and electrical properties were evaluated. Temperature dependencies of resistivity of ECNs carbonized at several temperatures were investigated. The character of the temperature dependencies of resistivity was typical for semiconducting materials. The values of corresponding activation energies were obtained for ECN samples carbonized at different temperatures, and the results showed that the activation energy of ECNs decreased with the increase of carbonization temperature.

Carbon nanofibers can be prepared through thermal treatments (i.e., stabilization and carbonization) of electrospun polyacrylonitrile (PAN) nanofibers as the precursor [1]. Unlike carbon nanotubes/nanofibers that are produced by bottom-up synthetic methods, electrospun carbon nanofibers (ECNs) are produced through a top-down nano-manufacturing process; this results in low-cost, and more importantly, continuous nanofibers that are easy to align, assemble, and process into applications. In addition to conventional applications such as reinforcement fillers in composites, ECNs also possess the potential to be used as the sensing elements and/or building blocks for the fabrication of electronic and/or photonic devices. It is vital, therefore, to understand the electrical properties of these materials [2–6]. The purpose of this research is to study the electrical properties of various ECNs prepared from electrospun PAN nanofibers with different temperatures of carbonization. Our measurements showed that the resistivity of ECNs decreased exponentially with the increase of carbonization temperature, thus indicating that the ECNs possessed the semiconductor type of conductivity. The activation energies of charge transport extracted from temperature dependencies of resistivity were obtained for ECNs carbonized at varied temperatures.

For the preparation of ECNs, the PAN microfibers of S.A.F. 3 K (Courtaulds, UK) were first dissolved in *N*,*N*-dimethylformamide at 60 °C to make a 14 wt% solution. The detailed procedures and conditions for electrospinning were described in a previous publication [7]. The electrospun PAN nanofibers were then stabilized at 250 °C for 6 h in air (the rate of temperature increase was 1 °C/min); subsequently, the stabilized nanofibers were carbonized at the temperatures of 600, 650, 700, 800, 900, 1200, and 1400 °C (the rate of temperature increase was 5 °C/min) in argon (the argon flow rate was 1 cubic foot per hour). The samples were held at the carbonization temperatures for 1 h before being cooled to room temperature. Electrospun PAN nanofibers were white and could be easily separated into small tufts of fibers; the stabilized nanofibers were brown, while the carbonized nanofibers (i.e., ECNs) were black. The nanofibers in all of the samples were randomly overlaid.

N. Hedin · V. Sobolev · L. Zhang · Z. Zhu · H. Fong
South Dakota School of Mines and Technology, Rapid City, SD 57701, USA

V. Sobolev (✉)
Department of Physics, South Dakota School of Mines and Technology, 501 East St Joseph Street, Rapid City, SD 57701, USA
e-mail: Vladimir.Sobolev@sdsmt.edu

H. Fong (✉)
Department of Chemistry, South Dakota School of Mines and Technology, 501 East St. Joseph Street, Rapid City, SD 57701, USA
e-mail: Hao.Fong@sdsmt.edu

Morphologies of the samples were examined by the Zeiss Supra 40VP field-emission scanning electron microscope (SEM). The nanofibers in all of the samples were quite uniform with diameters of ~250 nm. The thicknesses of ECN samples (in the range from 60 to 100 μm) were measured using the obtained SEM images. The Rigaku Ultima Plus X-ray diffractometer (XRD), operating at 40 kV and 90 mA with the Cu Kα radiation (wavelength $\lambda = 0.154$ nm), was employed for the study; and the acquired XRD patterns for all of the ECNs were similar to the ones reported in literature [6, 8]. The average values of interplanar spacing (d_{002}), calculated using the Bragg equation, were ~0.355 nm; while the average sizes of graphite crystallites (L_c), determined using the Scherrer equation, were in a range from 0.75 to 1.11 nm. We also conducted studies of ECN samples using a Renishaw RM2000 Raman spectrometer. An argon laser beam with the wavelength of 514.5 nm was used, the spot diameter was set at 5 μm, and the detector integration time was 30 s. The Raman spectra of ECNs demonstrated the gradual conversion from disordered carbonaceous components into ordered graphite crystallites with the increase of carbonization temperature similar to the reported results [8, 9]. The parameters characterizing the sizes of in-plane graphite crystallites (L_a) could be derived [9], using the Raman spectra data. For the ECN samples prepared at the carbonization temperatures of 600, 700, 800, and 1200 °C, the gradual increases of L_a parameter from 3.7 to 4.65 nm were observed.

Microstructures of ECNs were examined by the FEI Titan 80-300 scanning transmission electron microscope (STEM) operated at 300 kV. The TEM images at low and high magnifications are shown on the left and right sides of Fig. 1, respectively. It is noteworthy that ECNs were reduced to short fibers for the preparation of TEM specimens, while each image in Fig. 1 represents the typical microstructure. The ECNs carbonized at 600 °C had a high content of amorphous carbon; the ECNs carbonized at 700 and 1200 °C exhibited some graphitic crystalline content, and the graphitic crystalline content increased with the increase of carbonization temperature. It appeared that the crystalline structures started to emerge on the surfaces of fibers, and the crystalline layer thickened as the carbonization temperature increased. The ECNs carbonized at 1200 °C had a graphitic layer of ~5 nm. The information provided by the TEM images is consistent with that provided by the XRD and Raman results, as well as the published TEM images of similar materials [10, 11].

The electronic transport properties of individual PAN-based pregraphitic carbon nanofibers were investigated in a wide interval of temperatures from 5 to 300 K in a series of studies [4, 12–16]. It was demonstrated that the conductivity temperature dependence followed the Efros-Shklovskii variable-range hopping conductivity mechanism in this temperature interval [16]. Measurements of the room-temperature electrical conductivity on the ECN-based materials carbonized at different temperatures demonstrated the increase of room-temperature conductivity with increase of the carbonization temperature [8].

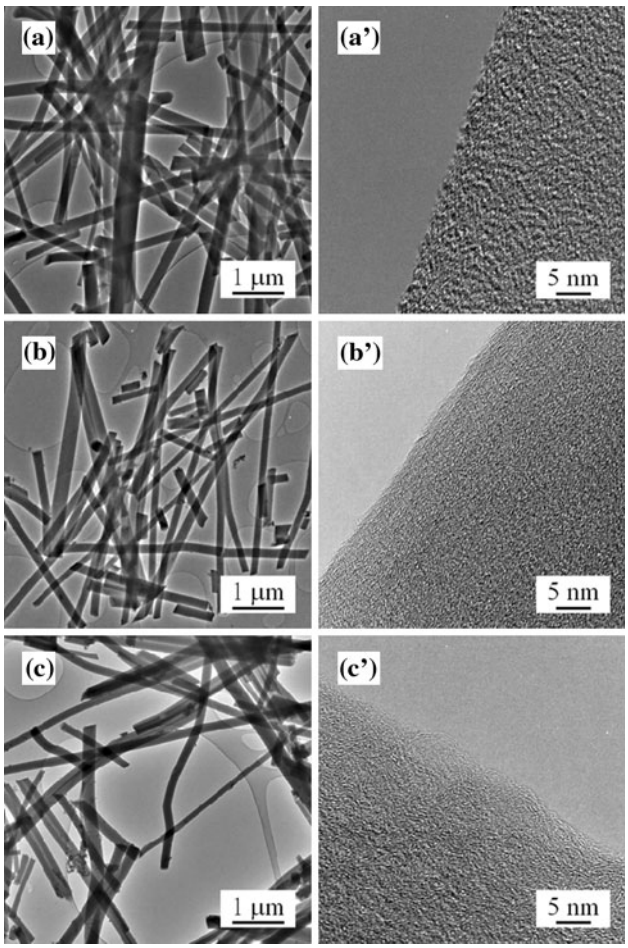

Fig. 1 TEM images of ECNs prepared at the carbonization temperatures of 600 °C (**a**), 700 °C (**b**), and 1200 °C (**c**). The images on the *left side* have low magnification (×3,800), while the ones on the *right side* have high magnification (×490,000)

Electrospun PAN nanofiber samples after stabilization at 220, 250, and 280 °C had resistances that were too high to measure by the equipment available to us. We carried out measurements of dielectric constants of these samples, using the QuadTech 7600 LCR meter and the Delta Design temperature control chamber. The dielectric constants for all of the stabilized samples were ~1.41, and they were nearly temperature independent within the interval from 25 to 175 °C.

The resistivity measurements were carried out on ECNs prepared through stabilization at 250 °C followed by carbonization at 600, 650, 700, 800, 900, 1200, and 1400 °C. The room-temperature resistance of the ECN samples

decreased by six orders of magnitude as the carbonization temperature increased from 600 to 1400 °C. We investigated the temperature dependencies of resistivity $\rho(T)$ of ECN samples in the temperature interval from 223 to 448 K (i.e., −50 to 175 °C), which is a common demand for the temperature range of stable operation for electronic devices. The *I–V* characteristics were measured by standard four-probe method using the Keithley 2600 SourceMeter and the measuring cell made by Jandel. The resistivity of the samples was calculated using the formula

$$\rho = \frac{\pi t}{\ln 2}\left(V/I\right),$$

where t is the sample thickness, V and I are measured voltage and current (see, for example, Ref. [17]). This formula was adopted because the thickness of all samples was much less than the distance between the contacts in four-probe cell. The ratio of *V*/*I* was obtained as slope of the linear part of the *I–V* characteristics for ECN samples at different temperatures in the temperature interval from −50 to 175 °C.

Dependencies of natural logarithms of resistivity on inverse temperature are presented in Fig. 2 for ECNs. The linear dependence of the natural logarithm of resistivity upon the inverse temperature is characteristic for materials with semiconducting type of conductivity. Assuming the exponential dependence of resistivity on temperature

$$\rho(T) \propto \exp\{E_g/(k_B T)\}$$

where E_g is the activation energy and k_B is the Boltzmann constant, the values of the activation energy for ECN samples carbonized at different temperatures can be obtained. The dependence of the activation energy on the carbonization temperature of samples is given in Fig. 3. It is evident that the activation energy of the ECN-based materials decreases with the increase of the carbonization temperature.

In summary, various ECNs were prepared through stabilization and carbonization of electrospun PAN nanofibers at different temperatures; and their morphological, structural, and electrical properties were evaluated. The ECNs had diameters of ~250 nm, and their graphitic crystallinity increased with the increase of carbonization temperature. The studies on temperature dependencies of resistivity demonstrated that the ECNs carbonized at the temperature from 600 to 1400 °C manifested the semiconducting type of conductivity. Based upon the results of studies on conductivity of individual carbon nanofibers [12–16], it is

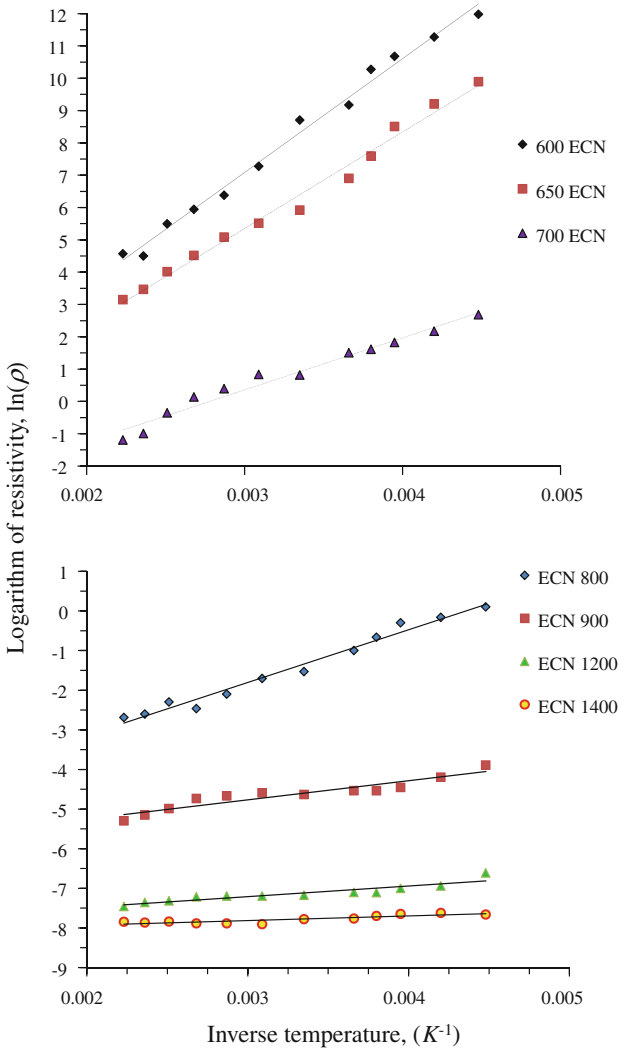

Fig. 2 Dependencies of natural logarithms of resistivity on inverse temperature for ECNs carbonized at the temperatures of 600, 650, and 700 °C (*top*), as well as 800, 900, 1200, and 1400 °C (*bottom*)

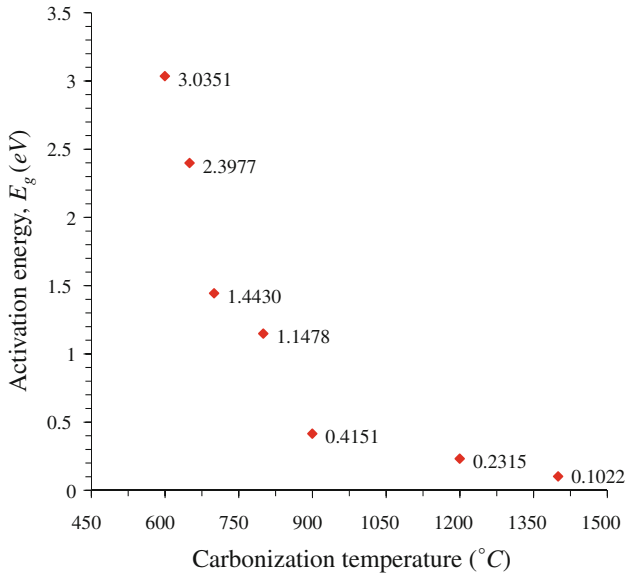

Fig. 3 Dependence of activation energy (E_g) in temperature dependence of resistivity $\rho(T) \propto \exp\{E_g/(k_B T)\}$ on the carbonization temperatures for ECN samples

expected that the conductivity of ECN-based materials will be determined by the combination of conductivity mechanisms characteristic for individual nanofibers with essential influence of the resistive properties of contact points among individual nanofibers [18]. It is noteworthy that the parameter E_g in the expression for temperature dependence of resistivity is related to the band gap in the electronic structure of the material in question. It is hard to clarify the actual relation at this stage of our studies without more detailed information about the main mechanisms of conductivity of ECN-based materials. However, it is intriguing to note that the ECN-based materials carbonized at the temperatures of 900, 1200, and 1400 °C had values of activation energy that are characteristic for the narrow-gap semiconductors, which make such materials interesting for the application in narrow-gap semiconducting photodiodes.

Acknowledgements This research was supported by the National Aeronautics and Space Administration of the United States (Grant No. NNX07AT52A). The authors wish to express their gratitude to Dr. Robert Corey for helpful discussions and to Mr. Gregory Serfling for his help with measurements of dielectric constant.

References

1. Liu J, Yue Z, Fong H (2009) Small 5:536
2. Morozowski S (1979) J Low Temp Phys 35:291
3. Duan X, Huang Y, Cui Y, Wang J, Leiber CM (2001) Nature 409:66
4. Wang Y, Ramos I, Furlan R, Santiago-Avilés JJ (2003) IEEE Trans Nanotechnol 2:39
5. Morgan PE (2005) Carbon fibers and their composites. CRC Press, Boca Raton, FL, pp 185–267
6. Song C, Wang T, Qiu Y, Qiu J, Cheng H (2009) J Porous Mater 16:197
7. Lai C, Zhong G, Yue Z, Chen G, Zhang L, Vakili A, Wang Y, Zhu L, Liu J, Fong H (2011) Polymer 52:519
8. Panapoy M, Dankeaw A, Ksapabutr B (2008) Thammasat Int J Sci Technol 13:11
9. Wang Y, Serrano S, Santiago-Avilés JJ (2003) Synth Met 138:423
10. Zhou Z, Liu K, Lai C, Zhang L, Li J, Hou H, Reneker DH, Fong H (2010) Polymer 51:2360
11. Liu F, Wang H, Xue L, Fan L, Zhu Z (2008) J Mater Sci 43:4316. doi:10.1007/s10853-008-2633-y
12. Wang Y, Serrano S, Santiago-Avilés JJ (2002) J Mater Sci Lett 21:1055
13. Wang Y, Ramos I, Furlan R, Santiago-Avilés JJ (2004) IEEE Trans Nanotechnol 3:80
14. Wang Y, Santiago-Avilés JJ (2004) IEEE Trans Nanotechnol 3:221
15. Wang Y, Santiago-Avilés JJ (2006) Appl Phys Lett 89:123119
16. Wang Y, Santiago-Avilés JJ (2003) J Appl Phys 94:1721
17. Schroder DK (2006) Semiconductor material and device characterization. Wiley-IEEE Press, Hoboken, NJ
18. Foygel M, Morris RD, Anez D, French S, Sobolev V (2005) Phys Rev B 72:104201